Supplement of Biogeosciences, 22, 6369–6392, 2025 https://doi.org/10.5194/bg-22-6369-2025-supplement © Author(s) 2025. CC BY 4.0 License.





## Supplement of

## Hot spots, hot moments, and spatiotemporal drivers of soil $\mathbf{CO}_2$ flux in temperate peatlands using UAV remote sensing

Yanfei Li et al.

Correspondence to: Yanfei Li (yanfei.li@uclouvain.be)

The copyright of individual parts of the supplement might differ from the article licence.

## S1. UAV campaigns

1

2

3

4

5

6

7

8

9

10

11

12

13

14

15

16

17

18

19

20

21

22

23

24

25

26

27

28

29

The UAV flight missions were carried out between 10 h 00 and 14 h 00, at a frequency of every two weeks in summer and monthly interval in other seasons. The flight patterns and altitudes used for UAV missions were similar to our previous work (Li et al., 2024). The RGB images were captured at a flight height of 100 m. The side and frontal overlap ratios were set to 70 % and 80 %, respectively, resulting in a spatial resolution of 2.05 cm. The multispectral and thermal infrared flights were conducted at above take-off point altitude of 90 m and a speed of 7.1 m/s simultaneously using a dual gimbal connector. Both side and frontal overlap ratios were set to 80 %. In this case, the spatial resolutions of the multispectral and thermal infrared images are approximately 6 cm and 12 cm, respectively. A MicaSense calibrated reference panel with known reflectance values was used immediately to calibrate the multispectral camera before and after each flight. The TeAX thermal infrared camera combines FLIR Tau2 cores and ThermalCapture hardware that allows the user to store raw infrared video streams directly on a local USB memory stick, together with additional information like position and time from GPS. In addition, TeAX technology makes heated shutters provide evenly a uniform temperature across the shutter and maintains this temperature throughout the duration of its operation. During the flight mission, the emissivity setting of the thermal infrared camera was set to 100 %. To further correct the differences between the true surface temperature of the ground and that measured by the sensor due to emissivity effect, two homemade thermal calibration panels (50 cm x 100 cm, one hot and one cold that fills with ice packs, Figure S2a) were used on the ground with a known temperature to adjust any offsets in the thermal images and to understand the temperature changes throughout the duration of the flight. To enhance the LiDAR signal penetration, we chose the triple-echo mode with a sampling frequency of 160 kHz, maintaining a flight height of 50 m above the take-off point at a speed of 6 m/s. During the flight mission, the ground sampling distances varied between 1.16 cm and 2.18 cm per pixel. The IMU calibration procedures were conducted automatically at the beginning, during the mission, and after flight routes to ensure inertial navigation accuracy. The RGB and LiDAR flights were conducted in RTK positioning mode using a D-RTK 2 base station (DJI, Shenzhen, China). The base station was set up at a known point and was used to provide real-time positional corrections throughout the flight. For the multispectral and thermal infrared cameras, nine ground control points (GCPs) were used (50 cm × 50 cm targets). The GCPs were made of white

- laminated board stuck with aluminum foil in the diagonal area and were distributed across the study site during the flight mission. Their position was measured using an Emlid Reach RS2 GPS device, utilizing a post-processing RTK solution with the Belgian WALCORS network.
- 33

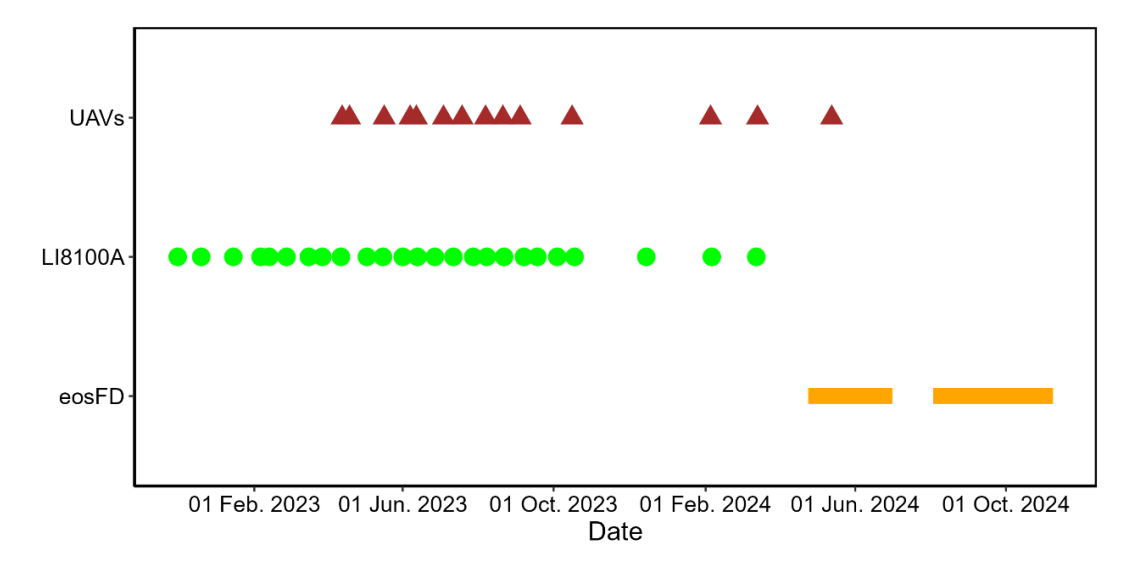


**Figure S1.** Dates of UAV flight missions, CO<sub>2</sub> flux measurements using the LI8100A system, and CO<sub>2</sub> flux measurements using the eosFD probes.

Hot panel

Thermometer sensor inside

Insulating foam

Cold panel

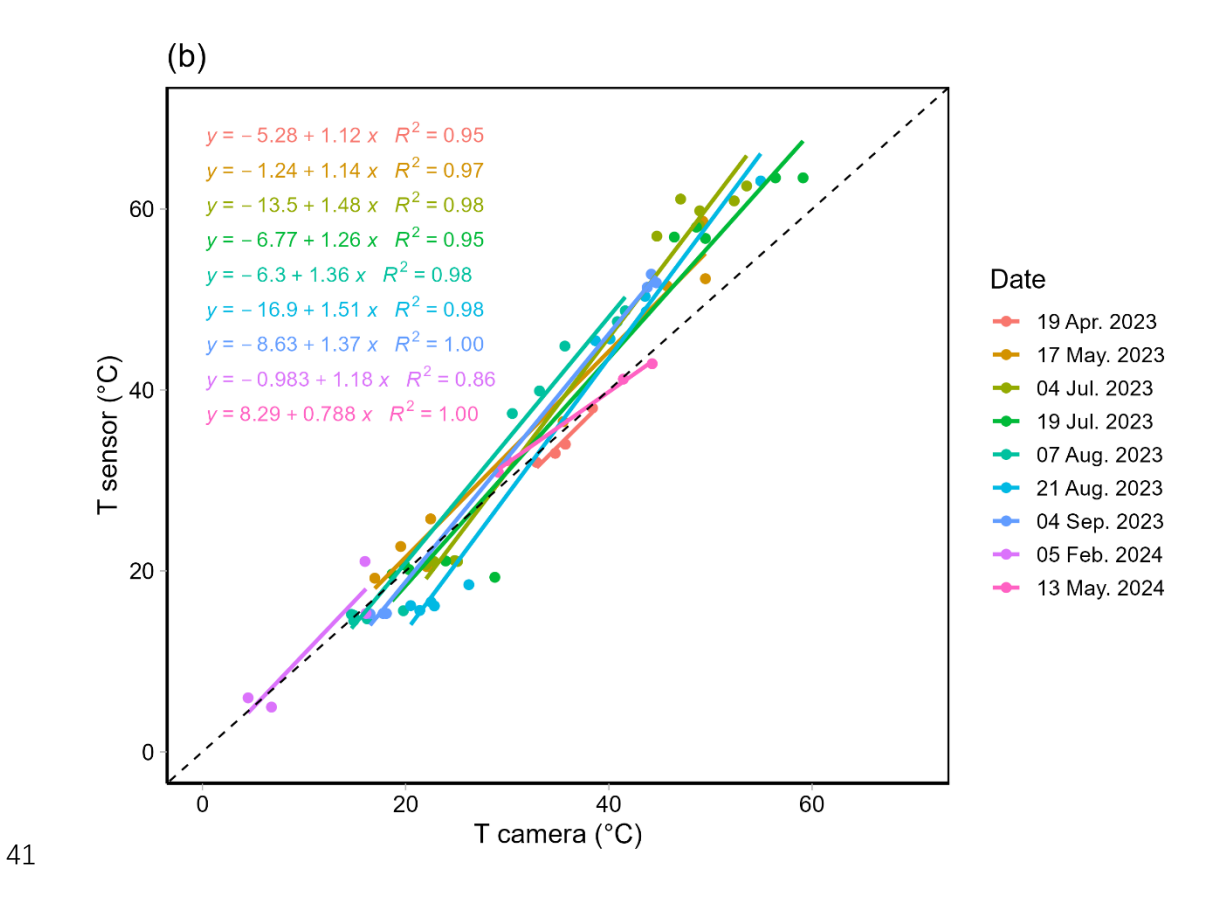
Metal sheet

Wooden frame

Ice pack placement area

Thermal infrared image

Hot panel



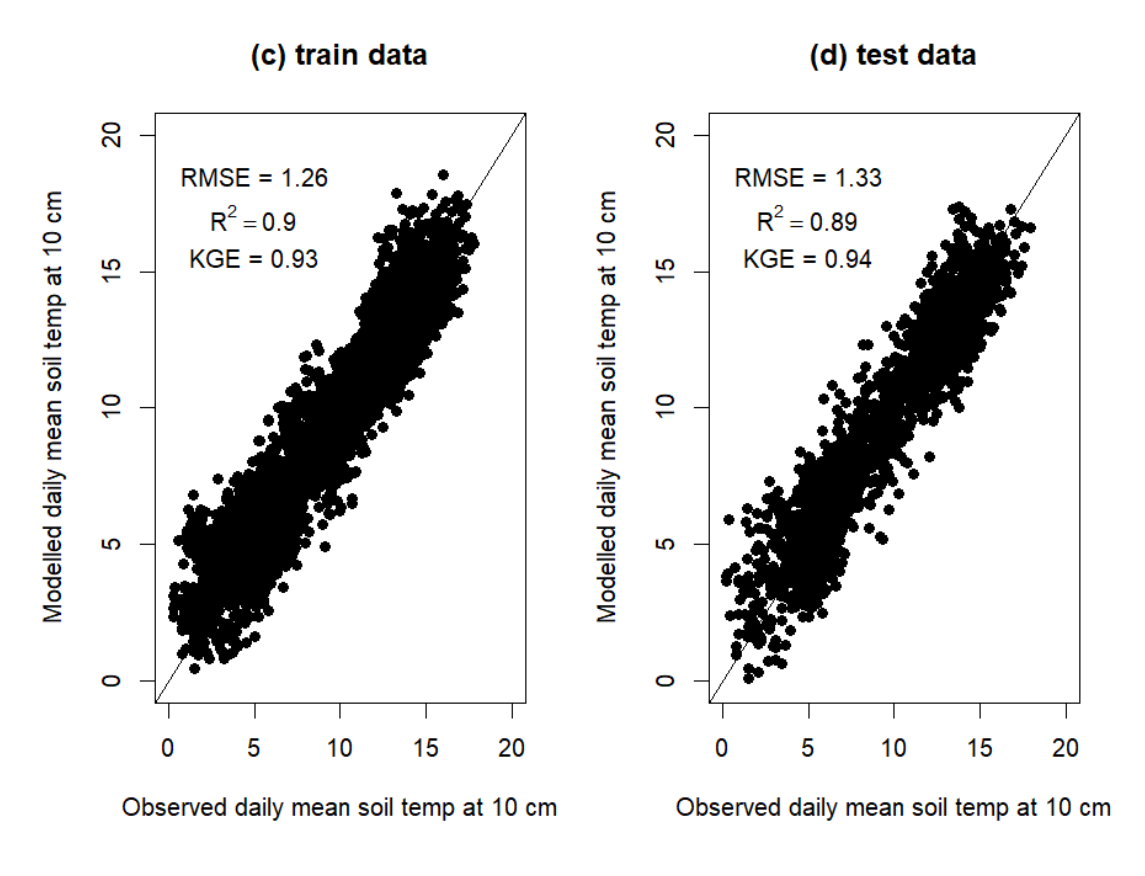
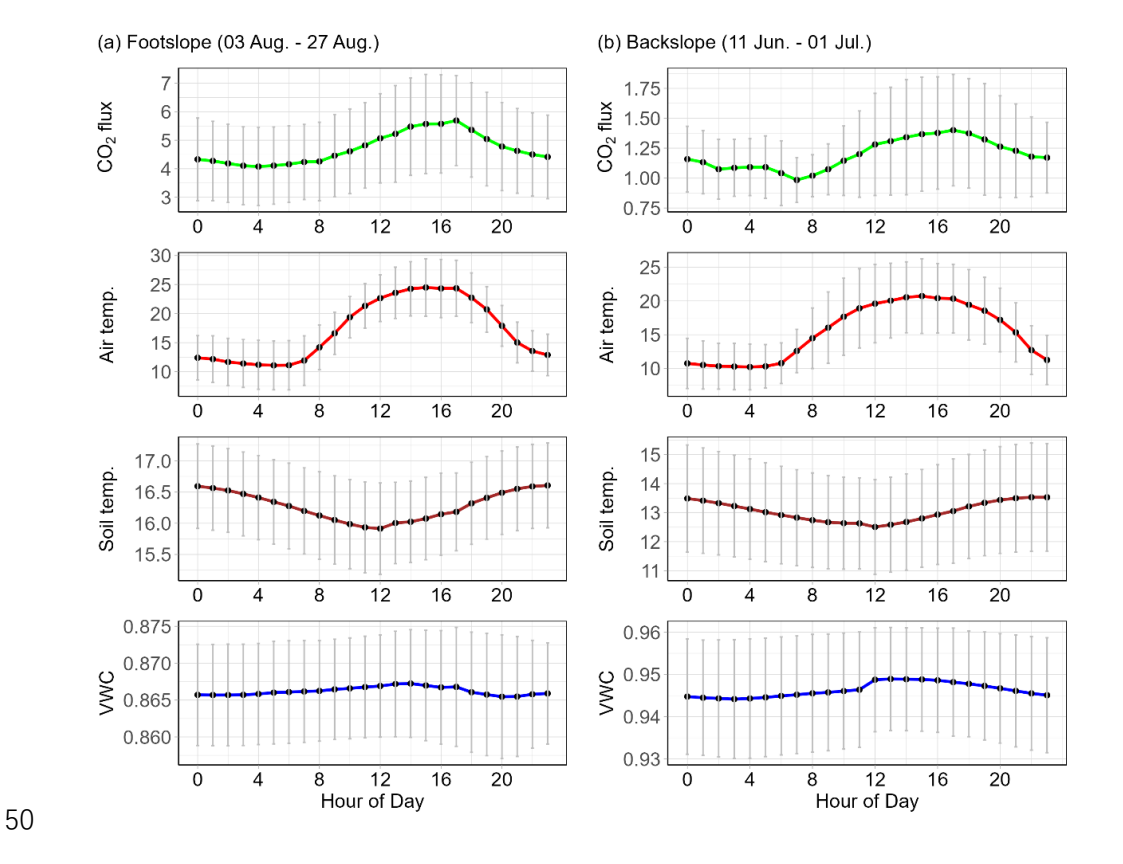


Figure S2. Experimental setup for thermal infrared data collection and an example thermal image showing the hot

and cold reference panels on 19 July 2023 (a). Comparison between thermometer-measured and camera-measured panel temperatures across different dates (b). Estimated daily mean soil temperature (at 10 cm depth) against observations using linear mixed-effects model (c) and (d). The corresponding RMSE and  $R^2$  values for the train and test datasets are annotated on the plot.



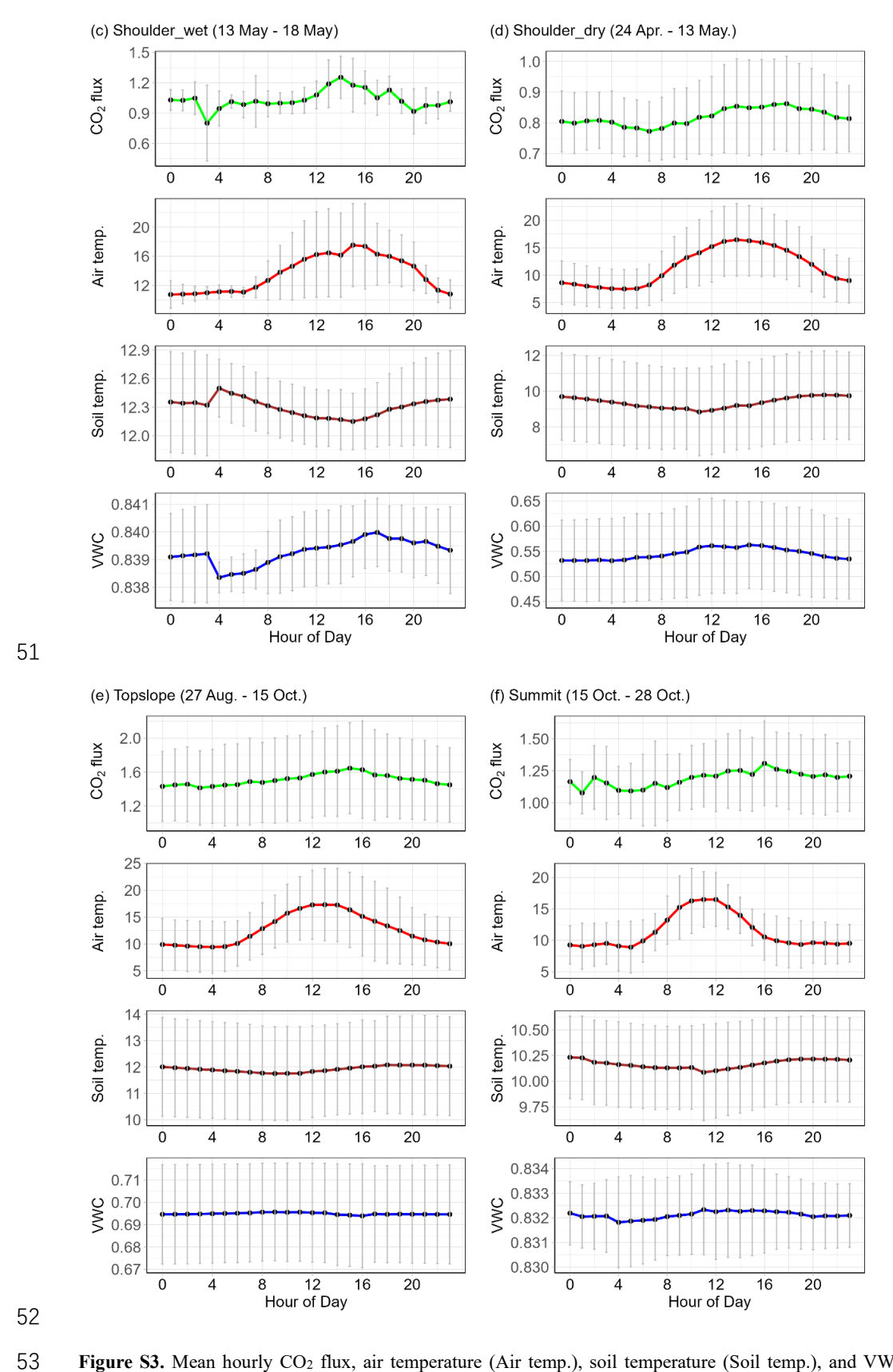
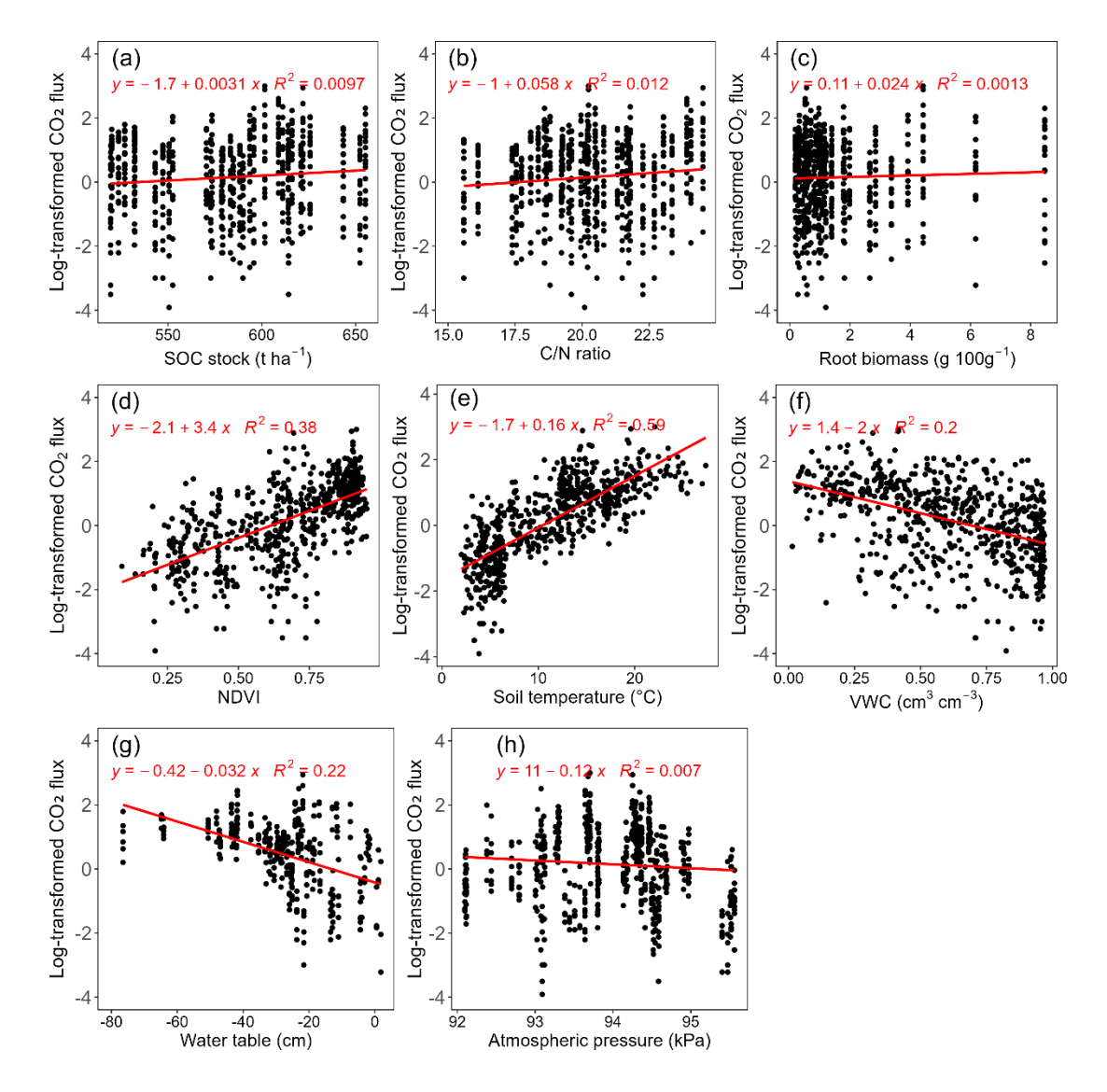


Figure S3. Mean hourly  $CO_2$  flux, air temperature (Air temp.), soil temperature (Soil temp.), and VWC across different slope positions. The  $CO_2$  data (unit:  $\mu$ mol m<sup>-2</sup> s<sup>-1</sup>) was based on measurements from the eosFD probes. Soil temperature (unit: °C) and VWC (cm<sup>3</sup> cm<sup>-3</sup>) were monitored at a depth of 10 cm using the Teros12 sensors. The air

temperature (unit: °C) was monitored at ~1.4 m above ground. The dot indicates the mean value, and the grey line (error bar) indicates the sd of each hour. The numbers of each subplot title indicate the monitoring period (Month/day).



**Figure S4.** Scatter plots showing relationships between log-transformed CO<sub>2</sub> flux and environmental variables: SOC stock (a), C/N ratio (b), root biomass (c), NDVI (d), soil temperature (e), soil VWC (c), water table (g), atmospheric pressure (h). The CO<sub>2</sub> fluxes were measured by the LI 8100A system.

	A in towns anotyms	0.32***
Fixed effects: Coefficients (contributions)	Air temperature	(39.31 %)
	NDVI	5.76***
	NDVI	(22.05 %)
	LST	0.21***
	LSI	(26.85 %)
Random effects	ICC	0.21
Kandom effects	(contributions)	(3.00 %)
M 11 C	Marginal R <sup>2</sup>	0.88
Model performance	Conditional R <sup>2</sup>	0.91
	AIC	16977.4
	RMSE	1.26
	KGE	0.93

70 Note. Significance level: \*\*\* p < 0.001, \*\* p < 0.01, \* p < 0.05.

**Table S2.** Coefficients and relative contributions of three types of input variables (static, semi-dynamic, dynamic) of mixed linear regression models for modelling seasonal patterns of  $CO_2$  flux at five slope positions (i.e., summit, topslope, shoulder wet, backslope, and footslope). Random effects were evaluated by *ICC* and model performance was evaluated by *Marginal R*<sup>2</sup>, *Conditional R*<sup>2</sup>, *AIC*, *RMSE*, and *KGE*.

	Input varia	ables	Model 1	Model 2	Model 3
Fixed effects:	Static	SOC stock	0.004*	0.004*	0.004*
coefficient		(t ha <sup>-1</sup> )	(2 %)	(2 %)	(2 %)
(contribution)		C/N ratio	0.04	0.05	0.05
			(2 %)	(2 %)	(2 %)
	Semi	root biomass	0.04	0.07	0.07
	dynamic	(g 100g <sup>-1</sup> )	(0.16 %)	(0.07 %)	(0.08 %)
		NDVI	2.29***	2.18***	2.18***
			(25 %)	(22 %)	(22 %)
	Dynamic	Soil temp.	0.06***	0.06***	0.06***
		(°C)	(24 %)	(21 %)	(21 %)
		VWC	-1.17***	-0.90***	-0.90***
		$(cm^3 cm^{-3})$	(17 %)	(13 %)	(13 %)
		Water table	\	-0.01**	-0.01***
		(cm)		(10 %)	(10 %)

	Atmospheric	\	\	-0.002
	pressure (kPa)			(1 %)
Random	ICC	0.21	0.23	0.23
effects	(contribution)	(7 %)	(6 %)	(6 %)
Model	Marginal R <sup>2</sup>	0.69	0.70	0.70
performance	Conditional $R^2$	0.76	0.76	0.76
	AIC	590.00	581.30	583.30
	RMSE	0.52	0.51	0.51
	KGE	0.82	0.82	0.82

Note. Significance level: \*\*\* p < 0.001, \*\* p < 0.01, \* p < 0.05. All CO<sub>2</sub> fluxes (unit:  $\mu$ mol m<sup>-2</sup> s<sup>-1</sup>), soil temperature, and VWC data for spatial and seasonal patterns were from the LI8100 A system. The water table data was from the Solinst probes at five slope positions and the atmospheric pressure data was from the meteorological station. The number of observations for modeling is 336.

## Reference

Li, Y., Henrion, M., Moore, A., Lambot, S., Opfergelt, S., Vanacker, V., Jonard, F., and Van Oost, K.: Factors controlling peat soil thickness and carbon storage in temperate peatlands based on UAV high-resolution remote sensing, Geoderma, 449, 117009, <a href="https://doi.org/10.1016/j.geoderma.2024.117009">https://doi.org/10.1016/j.geoderma.2024.117009</a>, 2024.